Lifetime of $1s2s2p\ {}^4P^o_{5/2}$ in V^{20+} using beam-foil techniques

T. Nandi,[1,*] P. Marketos,[2,†] P. Joshi,[1] R.P. Singh,[1] C.P. Safvan,[1] P. Verma,[3] A. Mandal,[1] A. Roy,[1] and R.K. Bhowmik[1]
[1]*Nuclear Science Center, Aruna Asaf Ali Marg, New Delhi-110 067, India*
[2]*FORTH - IESL, P.O. Box 1527, 71 110 Heraklion, Crete, Greece*
[3]*Vaish College, Rohtak, Haryana-124 001, India*
(Received 24 April 2002; published 26 November 2002)

A technique is developed for lifetime measurements of partially autoionizing levels using the time of flight method of the beam-foil and two-foil techniques at various beam energies. The decay curve of the 5.17-keV peak in heliumlike vanadium shows the presence of nonidentical decay constants in beam single-foil experiment in contrast to the growth structures in beam–two-foil measurements at different beam energies. Analysis of such data has not only confirmed the satellite blending problem of the $M2$ line $1s^2\ {}^1S_0$–$1s2p\ {}^3P^o_2$, but has also led to the mean lifetime measurement of the partially autoionizing satellite level of the $1s2s2p\ {}^4P^o_{5/2}$ line in lithiumlike vanadium. The lifetime so measured is compared with theoretical calculations.

DOI: 10.1103/PhysRevA.66.052510 PACS number(s): 32.30.Rj, 32.70.Fw, 31.30.Jv

I. INTRODUCTION

Reliable lifetime measurements provide a testing ground for understanding the wave function in atomic systems. The beam-foil time of flight technique is a unique method for measuring lifetimes in highly charged ions. However, this technique often suffers from cascade and blending problems which alter the observed lifetimes considerably. Experiments at different beam energies and a careful analysis may resolve these problems to a certain extent [1]. Lines originating from a doubly excited level of a given charge state of an ion are very close to the singly excited line in the next higher charge state. These are the satellite lines which for ions up to $Z=50$ are not resolved in solid state x-ray detectors commonly used in beam-foil experiments (for example, see Refs. [2,3]). The upper level of any satellite is partially autoionizing, and decay through both autoionization and radiative channels is possible. In the present work, we show that this property in conjunction with the two-foil technique enables the resolution of the satellite blending problem in the lifetime measurements of heliumlike vanadium ions. We have also made an attempt to measure the lifetime of the $1s2p\ {}^3P^o_2$ level in heliumlike vanadium using both single-foil and two-foil targets of the beam-foil technique at various beam energies. Our study indicates that this technique could lead to a standard lifetime measurement technique for the satellite levels for $Z=17$–40. In this paper we describe the technique and the analysis.

II. EXPERIMENT AND OBSERVATIONS

The ^{51}V ions at energies of 100 and 158 MeV used in the measurements were obtained from the 16MV Pelletron accelerator at the Nuclear Science Center, New Delhi. The beam passed through a 3-mm-diameter collimator onto the two-foil setup consisting of a 35-μg/cm^2 carbon foil followed by a second 4-μg/cm^2 foil. The second foil thickness was chosen so as to fulfill only single collision condition in the foil. The thinner carbon foil was kept fixed and the first foil was moved using a plunger system [8] controlled by microstepper motors. The distance between the foils could be varied in the range 0.115–10 mm, and the positioning accuracy was about 0.5 μm. X rays emitted by the foil-excited ions in a narrow zone a few mm downstream of the fixed carbon foil passed through a collimating system consisting of three slits as well as an x-ray shielding cup, and were detected by a low energy Germanium detector (resolution of 160 eV at 5.9 keV) placed at right angles to the beam direction. However, the resolution worsened to 195 eV due to Doppler broadening. The dimensions of the first slit (1.0×8 mm^2) were chosen to ensure that only the delayed x rays from foil-excited ions reached the detector. This was checked for the entire travel by replacing the movable carbon foil by a gold foil. Au x rays emanating from the foil were not observed in the spectra, thus confirming good x-ray collimation. The beam was collected by an unsuppressed Faraday cup built within the plunger. The thin foil was removed during the single foil experiment. The experimental geometry shown in Fig. 1 is similar to the beam-two-foil experiment of Cheng *et al.* [9]. An additional feature of this measurement was the normalization of the incident flux through elastic scattering of the beam from a 120-μg/cm^2 gold foil placed 20 mm downstream. Two silicon surface barrier detectors

TABLE I. Possible unresolved lines at 5.17-KeV. Theoretical transition energies are taken from Refs. [4,5]. Lifetimes are obtained from Refs. [2,6,7].

Ion	Line	Energy (keV)	Lifetime (ps)
V^{21+}	$1s^2\ {}^1S_0$–$1s2p\ {}^3P^o_0$	5.1758	91 [6]
V^{20+}	$1s^2 2s\ {}^2S_{1/2}$–$1s2s2p\ {}^4P^o_{5/2}$	5.1423	157 [7]
V^{21+}	$1s^2\ {}^1S_0$–$1s2p\ {}^3P^o_2$	5.1857	313 [6]
V^{21+}	$1s^2\ {}^1S_0$–$1s2p\ {}^3P^o_{11/2,3/2}$		313 [2]
V^{21+}	$1s^2\ {}^1S_0$–$1s2p\ {}^3P^o_{9/2}$		205 [2]
V^{21+}	$1s^2\ {}^1S_0$–$1s2p\ {}^3P^o_{7/2}$		202 [2]
V^{21+}	$1s^2\ {}^1S_0$–$1s2p\ {}^3P^o_{5/2}$		239 [2]
V^{21+}	$1s^2\ {}^1S_0$–$1s2s\ {}^3S_1$	5.15411	16.9 ns [2]

*Corresponding author. Email address: nandi@nsc.ernet.in
†Present address : SELETE, 141 21 N. Iraklion, Attiki, Greece

 ©2002 The American Physical Society

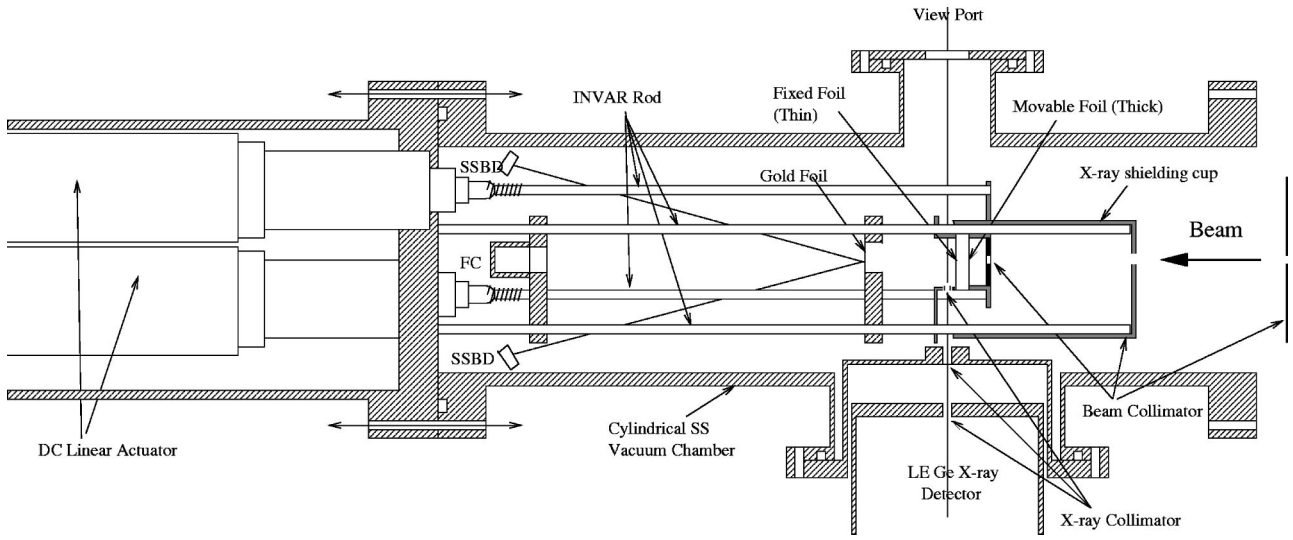

FIG. 1. Schematic of the experimental setup (not to scale).

placed symmetrically about the beam axis monitored the elastically scattered projectiles.

Due to the few mm distance between the foil and the detector, the fast $E1$ decays from the excited ions cannot reach the detector and were not observed. However, several lines originating from the metastable states as shown in Table I and Fig. 2, would reach the detector and these could not be resolved in the Ge detector spectrum. Since the unresolved lines have different mean lifetimes, all six time components (considering quenched heliumlike $1s2p\ ^3P^o_2\ F=7/2$ and 9/2 hyperfine levels together) need to be included in a full fit of the decay of the observed line. All these states of heliumlike vanadium decay radiatively to the $1s^2\ ^1S_0$ ground state except the $1s2s2p\ ^4P^o_{5/2}$ state, which has a dominant autoionizing channel decaying to the $1s^2\ ^1S_0$ state in addition to a radiative channel to the $1s^22s\ ^2S_{1/2}$ state.

The spectrum exhibits two prominent spectral lines at 158 MeV. The x-ray line energies were calibrated using a standard ^{241}Am source. The peak at 5.17 keV may be attributed to all the unresolved lines tabulated in Table I. The line at 5.42 keV (Fig. 3, beam energy 158 MeV), which was not discernible at 100 MeV, may therefore be tentatively associated with a hydrogenlike vanadium line.

The decay curves for the 5.17-keV line at beam energies of 100 and 158 MeV are shown in Fig. 4 for the single-foil experiment. A simple simulation showed that time components (Table I), except $1s2s\ ^3S_1$, cannot be resolved with the standard beam-foil time of flight technique. Lifetimes determined by fitting the single-foil data with one exponent correspond therefore to effective lifetime. The effective lifetimes of 242 ± 5 and 161 ± 5 ps were obtained by fitting the 5.17-keV decay curve (Fig. 4) with a single exponent at 158 and 100 MeV, respectively (Table III).

This observed variation of the effective lifetime with the beam energy in the single-foil experiments may only be attributed to blending or to cascade effects, as hyperfine-induced effects do not depend on the projectile energy. To explore the cause of this variation, we repeated the measurements of the intensity variation of the 5.17-keV peak using a two-foil carbon target [9]. A rise in intensity at 5.17 keV as the separation between the two foils increases is a distinctive feature of the spectra at 158 MeV (Fig. 3). As a result, a growing function appears clearly in the corresponding decay curve (Fig. 5). In contrast, the 100-MeV decay curve exhibits an initial decrease in intensity, followed by a constant value as the separation between the foils increases. We now discuss the possible origin of these observations.

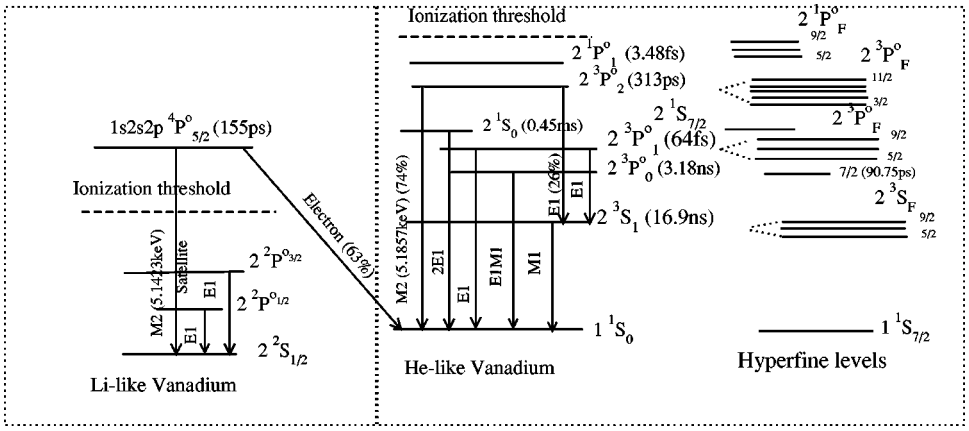

FIG. 2. Level scheme of lithiumlike and heliumlike vanadium ions is shown including the hyperfine levels in heliumlike vanadium ions. Theoretical lifetimes and branching ratios [5,6,10,11] are also given for selected levels.

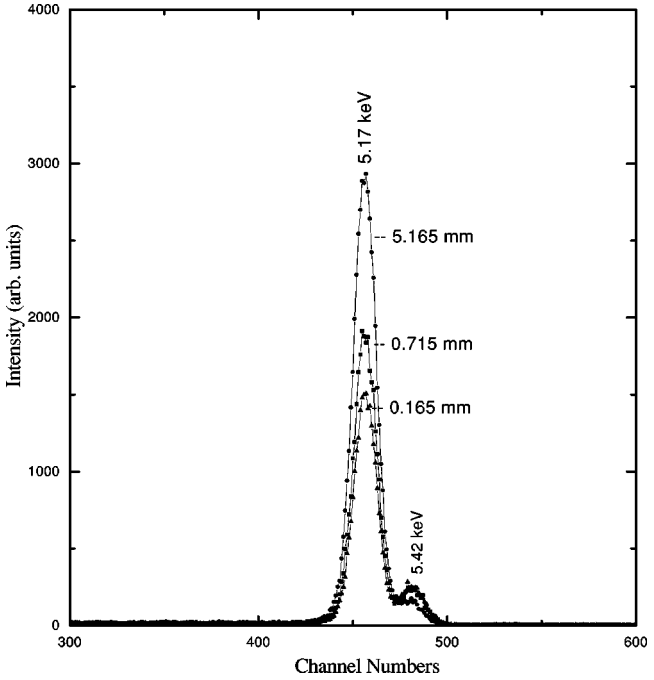

FIG. 3. X-ray spectra obtained using a two-foil carbon target, for three different foil separations at 158 MeV. The detector was kept at 5.6 mm from the second foil.

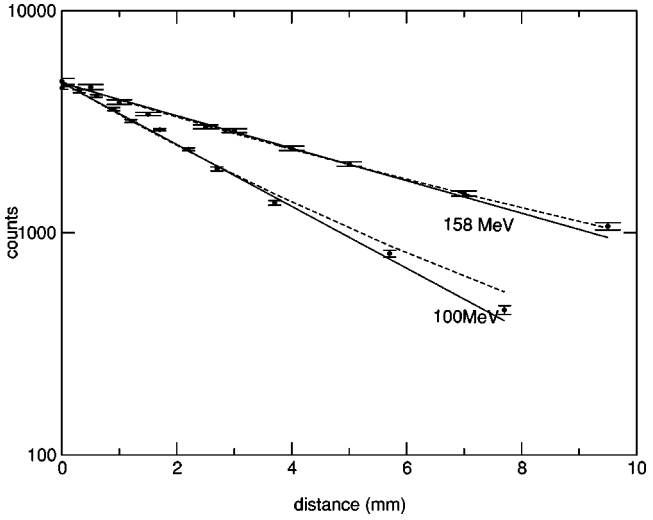

FIG. 4. Decay curve for 5.17-keV peak from the single-foil experiment. Normalized count rate vs distance between the target foil and the detector for the 5.17-keV vanadium line. The foil to detector slit distance was 5.6 mm in the 158-MeV experiments and 2.3 mm in the 100-MeV experiment. The solid lines were obtained by fitting the data using a single exponent, the dashed lines using two exponents.

III. DATA ANALYSIS, RESULTS, AND DISCUSSIONS

In the two-foil situation, we focus on the excitation-deexcitation processes of the ions in two regions, viz., (i) the variable foil separation x between two foils, and (ii) the fixed distance d between the second foil and the detector slit. The deexcitation phenomenon in x is identical to the single foil situation. However, due to interaction with the second foil the relative intensity of each decay component may be altered, and as a result the effective lifetime may differ considerably. All the levels decaying radiatively can be represented with $I_1' e^{-x/v\tau_1} e^{-d/v\tau_1'}$. Here τ_1' is the effective lifetime but different from τ_1 as the relative strengths of the various time components change due to the interactions in the second foil. Although the lifetime τ_1' ought to change for every value of x, we approximate it to a fixed value at this stage. A heliumlike vanadium ground state, produced from the photon decay of all the states, might have a certain probability to reproduce any of these states (Table I). Therefore, it leads to a growth term of $I_1''(1-e^{-x/v\tau_1})e^{-d/v\tau_1''}$, where τ_1'' is a fixed effective lifetime containing different strengths of all six states produced due to the interaction of the heliumlike vanadium ground state and the second foil. τ_1' may not differ much from τ_1''. The autoionizing $1s2s2p\ ^4P^o_{5/2}$ lithiumlike vanadium level decays through both autoionization as well as radiative processes, and the branching ratio for the autoionizing channel is rather large (63% [11] and 65.7% [12]). The ground state of heliumlike vanadium produced at x, due to the autoionizing transition $1s^2\ ^1S_0 - 1s2s2p\ ^4P^o_{5/2}$, can generate all the six states due to the interaction in the second foil. Therefore, it contributes to a growth term as $I_2'(1-e^{-x/v\tau_2})e^{-d/v\tau_1''}$, where τ_2 is the pure lifetime of $1s2s2p\ ^4P^o_{5/2}$. Interestingly, the $1s2p\ ^3P^o_2$ state has an $E1$ branch (Fig. 1) to $1s2s\ ^3S_1$ which could regenerate the $1s2s2p\ ^4P^o_{5/2}$ level while passing the second foil by capturing an electron in the $2p$ shell. Such an electron capture

TABLE II. Processes at the second foil that lead to the various terms in Eq. (3.3) (see the text). The excited levels giving rise to unresolved transitions are given in Table I. In the single foil data these levels are associated with an effective lifetime.

Levels before the second foil	Levels after the second foil	Intensity component
All excited levels giving rise to unresolved transitions, $1s^2$ from radiative decay of those levels	All excited levels giving rise to unresolved transitions	I_1, I_5
$1s^2$ from autoionization of $1s2s2p\ ^4P^o_{5/2}$	All excited levels giving rise to unresolved transitions	I_2
$1s2s\ ^3S_1$ arising from $1s2p\ ^3P^o_2$	$1s2s2p\ ^4P^o_{5/2}$, by electron capture	I_3
$1s2s\ ^3S_1$	$1s2p\ ^3P^o$, by spin flipping	I_4

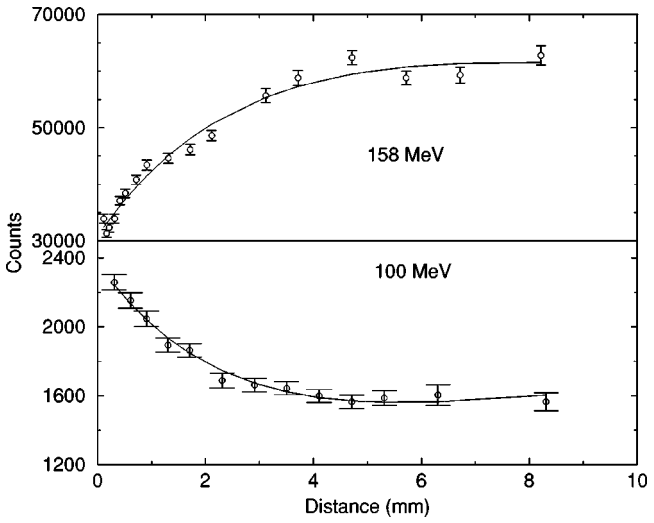

FIG. 5. Two-foil experiment. Normalized count rate vs distance between the two foils for the 5.17-keV vanadium line. The detector was kept at a distance of 5.6 mm from the second foil for the 158-MeV experiment (upper curve) and at 4 mm for the 100-MeV experiment (lower curve). The solid lines are the fits to the data.

process results in another growing term $I_3'(1-e^{-x/v\tau_3})e^{-d/v\tau_2}$, where τ_3 is the lifetime of the $1s2p\ ^3P_2^o$ (including all hyperfine levels). It may be noted that the $1s2p\ ^3P_2^o$ and $1s2s\ ^3S_1$ states decaying to the $1s^2\ ^1S_0$ state will have to undergo both excitation and capture within the second foil, which is very unlikely in a single collision condition [13]. Further, there is a certain probability of a long lived $1s2s\ ^3S_1$ state exchanging with a triplet-p states and vice versa [9]. This would also lead to a growing component as $I_4'(1-e^{-x/v\tau_4})e^{-d/v\tau_4'}$, where τ_4 is 16.9 ns, and τ_4' is an effective and fixed lifetime which may be different from τ_4 because the resultant state is a mixture of triplet-s and triplet-p levels [9]. Cascades to all the six levels are very fast [5] and the effect may be ignored without introducing any significant error. Now adding all the terms together,

$$I(x)=I_1'e^{-x/v\tau_1}e^{-d/v\tau_1'}+I_1''(1-e^{-x/v\tau_1})e^{-d/v\tau_1''}+I_2''(1-e^{-x/v\tau_2})e^{-d/v\tau_1''}+I_3'(1-e^{-x/v\tau_3})e^{-d/v\tau_2}+I_4'(1-e^{-x/v\tau_4})e^{-d/v\tau_4'}. \quad (3.1)$$

Rearranging the first and second terms of the above equation, we obtain

$$I(x)=e^{-x/v\tau_1}(I_1'e^{-d/v\tau_1'}-I_1''e^{-d/v\tau_1''})+I_1''e^{-d/v\tau_1''}+I_2''(1-e^{-x/v\tau_2})e^{-d/v\tau_1''}+I_3'(1-e^{-x/v\tau_3})e^{-d/v\tau_2}+I_4'(1-e^{-x/v\tau_4})e^{-d/v\tau_4'}. \quad (3.2)$$

Since the second foil is held fixed, all the terms not involving x are constant for a given velocity. Thus, redefining the intensity parameter $(I_1'e^{-d/v\tau_1'}-I_1''e^{-d/v\tau_1''})$ as I_1, $I_1''e^{-d/v\tau_1''}$ as I_5, $I_2''e^{-d/v\tau_1''}$ as I_2, $I_3'e^{-d/v\tau_2}$ as I_3, and $I_4'e^{-d/v\tau_4'}$ as I_4, Eq. (3.2) takes the form

$$I(x)=I_1e^{-x/v\tau_1}+I_2(1-e^{-x/v\tau_2})+I_3(1-e^{-x/v\tau_3})+I_4(1-e^{-x/v\tau_4})+I_5. \quad (3.3)$$

The terms in Eq. (3.3) give only the contributions occurring during the flight in the separation between the two foils.

The origin of each component of Eq. (3.3) is summarized in Table II.

In the total contribution, there are three growing components, viz., $1s2s2p\ ^4P_{5/2}^o$ (τ_2), $1s2p\ ^3P_2^o$ (τ_3), and $1s2s\ ^3S_1$ (τ_4) having theoretical lifetimes of 157 ps [7], 313 ps (without hyperfine quenching), or 258 ps (with hyperfine quenching) [14], and 16.9 ns [10], respectively. The measured effective lifetime from single-foil experiment is 242 ps. A growth of the counts in the two-foil experiment at 158 MeV at small separations indicates that the major growing component is faster than 242 ps. Thus the growing component of 157 ps may play a major role at this energy. We then assume that the 158-MeV two-foil data may be fitted with

TABLE III. Lifetimes for the $1s2p\ ^3P_2^o$ heliumlike and $1s2s2p\ ^4P_{5/2}^o$ lithiumlike ^{51}V levels (ps). Nuclear charge is 23, nuclear spin 7/2, and a nuclear magnetic dipole moment $5.15141\mu_N$. The x-ray branching ratio for the $1s2s2p\ ^4P_{5/2}^o$ level is 37% [11] and 34% [12], and that for the $1s2p\ ^3P_2^o$ level is 74% [10].

Upper level	Beam energy (MeV)	Lifetime (ps) experiment (This work)	Lifetime (ps) theory
All six	158	242±5 [a]	
$1s2p\ ^3P_2^o$	158	322±28 [b]	
All six	100	161±5 [a]	
$1s2p\ ^3P_2^o$	100	306±32 [d]	
$1s2p\ ^3P_2^o$		314±21 [e]	310 [5,10], 313 [6] 242 [c] [6], 258 [c] [14]
$1s2s2p\ ^4P_{5/2}^o$	158	125±18 [f]	
$1s2s2p\ ^4P_{5/2}^o$	100	121±20 [g]	
$1s2s2p\ ^4P_{5/2}^o$		123±13 [h]	155 [11],159 [12] 157 [7]

[a]Single-foil data fitted with one exponent.
[b]Single-foil data fitted with two exponents of Eq. (3.5) (the lifetime of the $1s2p\ ^3P_2^o$ state was varied, and that of the $1s2s2p\ ^4P_{5/2}^o$ state was fixed to 125 ps).
[c]Including hyperfine quenching.
[d]Two-foil data fitted with Eq. (3.6) (the decay was fixed to 161 ps, and the growing component was varied).
[e]Average of the values obtained with the 158- and 100-MeV beams.
[f]Two-foil data fitted with Eq. (3.4) (the decay was fixed to 242 ps, and the growing component was varied).
[g]Single-foil data fitted with two exponents of Eq. (3.4) (the $1s2p\ ^3P_2^o$ state was fixed to 306 ps, and the $1s2s2p\ ^4P_{5/2}^o$ state was varied).
[h]Average of the values obtained with the 158- and 100-MeV beam.

$$I(x)=I_1e^{-x/v\tau_1}+I_2(1-e^{-x/v\tau_2})+I_5. \tag{3.4}$$

A least square fit of the two-foil data using the above equation was performed. In the fitting procedure, the effective lifetime τ_1 was fixed to the value (242 ps) obtained from the single foil measurement. The lifetime of the pure $1s2s2p\ ^4P^o_{5/2}$ level responsible for the growth is then determined to be 125 ± 18 ps (Table I). The best fit gave the values $I_1=37\%$ and $I_2=63\%$ with no contribution from I_5.

In order to disentangle the contribution of the $1s2s2p\ ^4P^o_{5/2}$ level from the effective lifetime determined from the decay of the 5.17-keV line in the single-foil situation, we repeated the analysis of the single-foil decay curve at 158 MeV. The decay curve was fitted with two exponents rather than one, as given by

$$I(x)=I_1e^{-x/v\tau_1}+I_2e^{-x/v\tau_2}. \tag{3.5}$$

In this fitting procedure, lifetime of the component associated with the satellite line, τ_1, was kept fixed at 125 ± 18 ps (Table I), and a 3σ error was considered so as to restrict the reduced χ^2 close to unity. The lifetime of the second component, τ_2, determined in this manner is 322 ± 28 ps and it may be attributed to the states $1s2p\ ^3P^o_{2,0}$, as our analysis is unable to eliminate the contribution of the $1s2p\ ^3P^o_0$ state. However, the closeness of this value to the expected value of 313 ps for the $1s2p\ ^3P^o_2$ state implies that this state is predominantly excited.

At 100-MeV beam energy the measured effective lifetime of 161 ± 5 ps in the single-foil target, and the appearance of a constant number of counts at large distances in the twofoil situation implies that the growing component must be slower than 161 ps. Among the components contributing to the 5.17-keV peak, major candidates are the $1s2p\ ^3P^o_2$ (200–313 ps including all hyperfine lines) and $1s2s\ ^3S_1$ states. Therefore, in the analysis Eq. (3.3) can be reduced to

$$I(x)=I_1e^{-x/v\tau_1}+I_3(1-e^{-x/v\tau_3})+I_4(1-e^{-x/v\tau_4})+I_5. \tag{3.6}$$

In the fitting procedure τ_1 was kept fixed at 161 ps and τ_3 was varied to determine the lifetime of the $1s2p\ ^3P^o_2$ state as 306 ± 32 ps. The intensity I_4 is found to be less than 1% with $I_5\approx0$, in contrast to $I_1=54.8$ and $I_3=44.7\%$. Next the single foil data were refitted using two exponents fixing one lifetime to 306 ps while varying two intensity parameters and one lifetime as in the case of 158-MeV data. This fitting resulted in a lifetime of 121 ± 20 ps for the second component and we may associate this value with the effective lifetime of $1s2s2p\ ^4P^o_{5/2}$ and $1s2p\ ^3P^o_o$ levels. This effective mean life may be interpreted to arise from contribution of the $1s2s2p\ ^4P^o_{5/2}$ and $1s2p\ ^3P^o_o$ levels of the order of 52% and 48%, respectively. The contribution of the $1s2p\ ^3P^o_o$ level is thus very different from that obtained from 158-MeV data. However, if we attribute the mean life of 121 ± 20 ps to the lifetime of the autoionizing state $1s2s2p\ ^4P^o_{5/2}$ alone, then the data at both 100 and 158 MeV are consistent. The lifetimes of the states $1s2p\ ^3P^o_2$ and $1s2s2p\ ^4P^o_{5/2}$, thus determined in this experiment, are 314 ± 21 and 123 ± 13 ps, respectively (see Table III).

TABLE IV. The relative level population I_{Li}/I_{He} of the $1s2s2p\ ^4P^o_{5/2}$ state is compared with respect to that of the $1s2p\ ^3P^o_2$ state at different beam energies and in different situations of single-foil as well as two-foil experiments. X-ray and autoionizing branching ratios of $1s2s2p\,^4P^o{}_{5/2}$ are taken from Refs. [11,12].

Beam energy (MeV)	Intensity ratio single-foil expt.	Intensity ratio two-foil expt.
100	11.67 [11], 12.7 [12]	11.28 [11], 11.28 [12]
158	5.89 [11], 6.4 [12]	6.45 [11], 5.79 [12]

We have assumed two different processes in determining the mean lives of $1s2p\ ^3P^o_2$ and $1s2s2p\ ^4P^o_{5/2}$ from the single- and two-foil data at two different beam energies. If the assumptions are appropriate, then the relative intensities of $1s2p\ ^3P^o_2$ (I_{He}) and $1s2s2p\ ^4P^o_{5/2}$ states I_{Li} in a single-foil situation must agree well with the two-foil case. An attempt was made to do so at both beam energies. With the assumptions made on the excitation mechanism in the thin second foil at 158 MeV, I_1 comprises a 74% intensity of the $1s2p\ ^3P^o_2$ state and a 37% intensity of the $1s2s2p\ ^4P^o_{5/2}$ state whereas I_2 is due to a 63% intensity of the $1s2s2p\ ^4P^o_{5/2}$ state. Therefore, the observed intensities from the fitting of two-foil data can be equated with the equation given below:

$$\frac{0.74I_{He}e^{-d/v\tau_1}+0.37I_{Li}e^{-d/v\tau_2}}{0.63I_{Li}e^{-d/v\tau_1}}=\frac{I_1}{I_2}. \tag{3.7}$$

Using the measured time components and equating these intensities with the observed intensities (I_1 and I_2) from the fitting with Eq. (3.4), we obtain the I_{Li}/I_{He} ratio. Similarly the equation used for the evaluating the I_{Li}/I_{He} in the single-foil case was

$$0.37I_{Li}e^{-d/v\tau_2}/0.74I_{He}e^{-d/v\tau_1}=I_1/I_2. \tag{3.8}$$

In this case, the observed intensities (I_1 and I_2) are obtained from fitting with Eq. (3.5).

Further, the observed intensities with two-foil data at 100 MeV were equated to Eq. (3.6) as

$$\frac{0.74I_{He}e^{-d/v\tau_1}+0.37I_{Li}e^{-d/v\tau_2}}{0.26I_{He}e^{-d/v\tau_1}}=\frac{I_1}{I_3}, \tag{3.9}$$

and the observed intensity ratios with single foil data with the same Eq. (3.8). The intensity ratios I_{Li}/I_{He} obtained in this manner are given in Table IV. Comparison of the data at two beam energies shows a very good agreement, validating the assumptions on the excitation mechanism. We have performed similar measurements at three beam energies for Ti and Ni, and the data support the present analysis very well for these cases.

The lifetime for the $1s2s2p\ ^4P^o_{5/2}$ state obtained in this experiment is much lower than that theoretically predicted [11,12,7]. Hyperfine quenching was considered responsible for the observed lower value of the lifetime [15]. The value of the lifetime of the $1s2p\ ^3P^o_2$ level measured in the present experiment is very close to the theoretical value without invoking hyperfine quenching [5,10]. Our measurement thus shows that the hyperfine quenched lifetime of the $1s2p\ ^3P^o_2$ level may be within the experimental uncertainty [15].

IV. CONCLUSION

We conclude by noting that lifetime measurements using the beam-foil technique with single-foil as well as two-foil target at different beam energies have been carried out for the first time in our laboratory to our knowledge. The present analysis shows that beam-foil and beam–two-foil experiments complement each other as far as satellite blending problem is concerned. Thus the present experimental approach and the analysis followed in the current study revealed the presence of blending due to the $1s^22s\ ^2S_{1/2}$–$1s2s2p\ ^4P^o_{5/2}$ satellite line in the measurement of the $1s2p\ ^3P^o_2$ lifetime. The mean lifetime of the $1s2s2p\ ^4P^o_{5/2}$ level of lithiumlike vanadium has been measured. This technique may be used for lifetime measurement of partially autoionizing satellite levels in lithiumlike ions ($Z=17$–40).

ACKNOWLEDGMENTS

We thank the Pelletron staff for providing the ion beam and R. Ram, D. Kabiraj, G. Mukherjee, S.C. Pancholi, B. Mukherjee, M.G. Vijaya, S.N. Soni, and S. Srivastava, for their help in various stages of the work. We gratefully thank C.V.K. Baba for useful discussions. T.N. and P.M. wish to thank U.I. Safronova and P. Indelicato for sharing useful data and I.P. Grant F.R.S. for providing the GRASP package.

[1] I. Martinson, Rep. Prog. Phys. **52**, 157 (1989).
[2] H. Gould, R. Marrus, and P.J. Mohr, Phys. Rev. Lett. **33**, 676 (1974).
[3] R.W. Dunford, C.J. Liu, J. Last, N. Beorrah-Mansour, R. Vondrasek, D.A. Church, and L.J. Curtis, Phys. Rev. A **44**, 764 (1991).
[4] T. Shirai, T. Nakagaki, J. Sugar, and W.L. Wiese, J. Phys. Chem. Ref. Data **21**, 273 (1992).
[5] I. P. Grant, C. F. Fischer, and F. A. Parpia, GRASP-1992 (private communication).
[6] W.R. Johnson, K.T. Cheng, and D.R. Plante, Phys. Rev. A **55**, 2728 (1997).
[7] M.H. Chen, B. Crasemann, and H. Mark, Phys. Rev. A **24**, 1852 (1981).
[8] P. Joshi, G. Mukherjee, A. Kumar, R.P. Singh, S. Muralithar, S.C. Pancholi, C.R. Praharaj, U. Garg, R.K. Bhowmik, and I.M. Govil, Phys. Rev. C **60**, 034311 (1999).
[9] S. Cheng, H.G. Berry, R.W. Dunford, D.S. Gemmell, E.P. Kanter, C. Kurtz, K.E. Rehm, and B.J. Zabransky, Phys. Rev. A **50**, 2197 (1994).
[10] J. Hata and I.P. Grant, Mon. Not. R. Astron. Soc. **211**, 549 (1984); T.W. Tunnell, C.P. Bhalla, and C. Can, Phys. Lett. A **75**, 195 (1980); C.D. Lin, W.R. Johnson, and A. Dalgarno, Phys. Rev. A **15**, 154 (1977).
[11] K. Cheng, C. Lin, and W.R. Johnson, Phys. Lett. A **48**, 437 (1974).
[12] U.I. Safronova, V.S. Senashenko, and I.A. Shavtvalishvili, Physika **12**, 13 (1977).
[13] J.H. McGuire, D.J. Land, J.G. Brennan, and G. Basbas, Phys. Rev. A **9**, 2180 (1979).
[14] P. Indelicato and G. Rodrigues (private communication).
[15] T. Nandi (unpublished).